# Torque Analysis and Improvement of Single-Phase Asymmetric-Stator-Pole Doubly Salient Permanent Magnet Machine

Mingjie He, Wei Xu, Caiyong Ye, and Dong Hu

State Key Laboratory of Advanced Electromagnetic Engineering and Technology, School of Electrical and Electronic Engineering, Huazhong University of Science and Technology, Wuhan 430074, China

**Doubly salient permanent magnet machine (DSPMM) has received extensive attentions recently due to its simple structure, high reliability, high torque density, etc. An improved 4/4 stator/rotor single-phase asymmetric-stator-pole DSPMM is proposed in this paper. First, it has investigated the topologies and operating principle based on torque expression and graphical description. Then, the effect of key structure parameters on torque is studied based on the 2-D finite-element algorithm. And then, comprehensive comparison on electromagnetic torque for the original and new machines is made. Finally, one prototype for the improved structure is manufactured and tested. It indicates that lower cogging torque, lower torque ripple, and stronger starting capability can be obtained by the improved structure. The theoretical results are well validated by comprehensive experiments.**

***Index Terms*— Cogging torque, finite-element algorithm (FEA), single-phase asymmetric-stator-pole doubly salient permanent magnet machine (SP-ASPDSPMM), starting torque, torque ripple.**

## I. Introduction

STATOR permanent magnet (PM) brushless machine has been studied extensively in recent years due to its high torque density, high efficiency, high reliability, low maintenance, etc., [1]–[6]. As one of the stator PM brushless machines, the doubly salient PM machine (DSPMM) has also attracted more and more attention [7]–[10]. However, the torque density of the traditional DSPMM with concentrated windings is limited by its unipolar flux linkage [7]. To obtain bipolar flux linkage and improve the electromagnetic performances, one 4/6 stator/rotor single-phase DSPMM with full-pitch winding configuration is developed in [8] and [9]. It could offer higher efficiency and lower copper cost with the same output power, but suffers from low material utilization ratio and poor starting performance.

To solve the problems mentioned earlier, one 4/4 stator/rotor single-phase asymmetric-stator-pole DSPMM (SP-ASPDSPMM) is proposed in [10]. Based on the analysis of [10], the torque density can be further improved by the SP-ASPDSPMM. But its torque ripple is relatively high, which may deteriorate its operation performance, and the starting torque is relatively low. Therefore, one improved SP-ASPDSPMM is presented in this paper, and the torque is investigated and compared with that of the original one.

This paper is organized as follows. In Section II, the topologies and operating principle of the SP-ASPDSPMMs are investigated. After that, the effect of key structure parameters on electromagnetic torque is studied based on the 2-D finite-element algorithm (2-D FEA) in Section III. In Section IV, the comparison of torque performance between the original and improved structures is made. Then, one prototype for the improved machine is made and tested in Section V. Finally, some conclusions are drawn in Section VI.

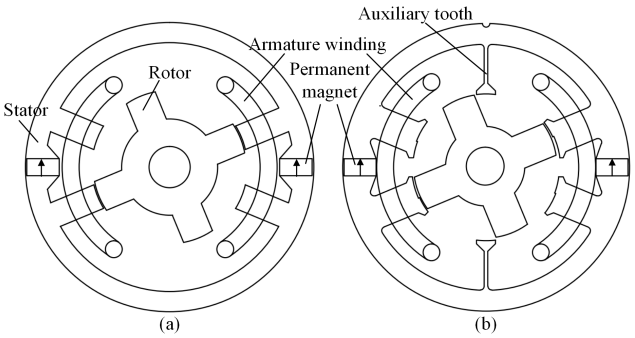


Fig. 1. Topologies and torque for both machines. (a) Original structure. (b) Improved structure.

## II. Topology and Operating Principle

### A. Topologies

The topology of the original machine is shown in Fig. 1(a), which contains stator and rotor with four poles, PMs, and armature windings. Its stator poles are distributed non-uniformly along the circumference, and the angle between two adjacent stator poles is 45°. Full-pitched armature windings are used and the rotor is similar to that of switched reluctance machine, which is rather simple and suitable for high-speed operation. Two circumferentially magnetized PMs are arranged on the stator yoke part and the magnetization directions of them are opposite. Compared with the original topology, the pole shoe, step air gap, and auxiliary teeth are introduced in the improved structure, as illustrated in Fig. 1(b).

### B. Operating Principle

The instantaneous torque produced by the proposed machine can be calculated in terms of the variation ratio of co-energy

Manuscript received March 9, 2018; revised April 10, 2018; accepted April 12, 2018. Corresponding author: C. Ye (e-mail: yecy@hust.edu.cn).

Color versions of one or more of the figures in this paper are available online at http://ieeexplore.ieee.org.

Digital Object Identifier 10.1109/TMAG.2018.2827951

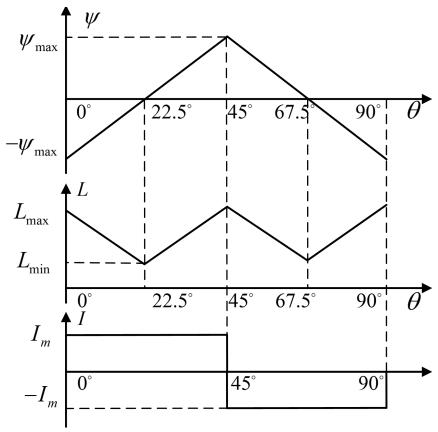


Fig. 2. Idealized PM flux, inductance, and current curves.

to rotor position, as given by

$$T = \left.\frac{\partial W'}{\partial \theta}\right|_{i=\text{const}} \tag{1}$$

where $W'$ is the co-energy, $i$ the instantaneous current, and $\theta$ is the rotor position.

Ignoring the saturation of iron core, the co-energy can be expressed by

$$W' = \psi i - \left(W_{\text{pm}} + \frac{1}{2}\text{Li}^2\right) = (\psi_{\text{pm}} + \text{Li})i - W_{\text{pm}} - \frac{1}{2}Li^2 \tag{2}$$

where $\psi_{\text{pm}}$ is PM flux, $L$ is the inductance, and $W_{\text{pm}}$ is the energy stored by the PMs.

Based on (1) and (2), the instantaneous torque can be obtained by

$$T = i\frac{\partial \psi_{\text{pm}}}{\partial \theta} + \frac{1}{2}i^2\frac{\partial L}{\partial \theta} - \frac{\partial W_{\text{pm}}}{\partial \theta} = T_{\text{pm}} + T_r - T_{\text{cog}} \tag{3}$$

where $T_{\text{pm}}$ is the interaction torque, $T_r$ is the reluctance toque, and $T_{\text{cog}}$ is the cogging torque. It is known that the instantaneous torque consists of three components: $T_{\text{pm}}$, $T_r$, and $T_{\text{cog}}$. As is known, $T_{\text{cog}}$ has no contribution to the average torque. As to $T_r$, it is related to the winding current and variation ratio of inductance versus rotor position, which has a positive value when the inductance goes up with rotor position. On the contrary, it would suffer a negative value. Thus, the average torque produced by $T_r$ in one whole conduction cycle could be zero and it has no contribution to the total average torque. Therefore, only $T_{\text{pm}}$ has contribution to the average toque, which is equal to the multiply of winding current and variation ratio of PM flux versus rotor position.

The idealized PM flux, inductance, and current curves are shown in Fig. 2. It is known that the positive current can be injected into the winding when the PM flux is increasing with rotor position to obtain positive average torque, while negative current injected when the PM flux is decreasing.

TABLE I
MAIN DESIGN SPECIFICATIONS

| Parameters | Values | Unit |
|---|---|---|
| Number of phase | 1 | - |
| Stator pole number | 4 | - |
| Rotor pole number | 4 | - |
| Rated power | 0.75 | kW |
| Rated speed | 25000 | rpm |
| Stator outer radius | 76/2 | mm |
| Stack length | 45 | mm |
| Air-gap length | 0.4 | mm |
| Rotor outer radius | 19 | mm |
| Width of PM | 8.5 | mm |
| Height of PM | 4.5 | mm |
| Width of stator pole | 8.5 | mm |
| Width of rotor pole | 9 | mm |
| Height of bridge | 0.3 | mm |
| Height of stator yoke | 5.5 | mm |
| Height of rotor yoke | 5.5 | mm |
| Iron core material | 50WW270 | - |
| PM material | N38UH | - |
| Turns of winding | 48 | - |

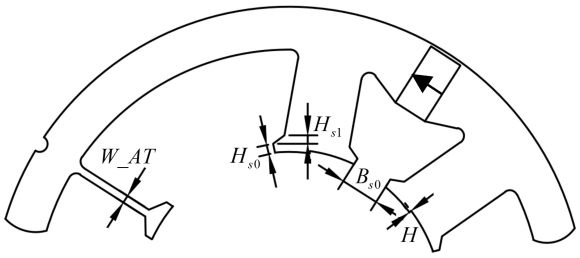


Fig. 3. Structure parameters.

## III. EFFECT OF STRUCTURE PARAMETERS ON ELECTROMAGNETIC TORQUE

### A. Design Restrictions and Parameters

To investigate the influence of designed structure parameters on torque performance indexes, including average torque, torque ripple, and starting torque, one prototype is designed based on the given restrictions and parameters, as shown in Table I and Fig. 3. The structure parameters of pole shoe, step air gap, and auxiliary teeth are selected for the following analysis. It is known that W_AT is the auxiliary teeth width, $H_{s0}$ is the slot opening height, $H_{s1}$ is the slot wedge height, $H$ is the height of stepped air gap, and $B_{s0}$ is the slot opening width.

### B. Slot Opening and Wedge Height

The curves of average and peak-to-peak torque versus slot opening and wedge height are shown in Fig. 4. It indicates that the average and peak-to-peak torque would decrease with the increasing of $H_{s0}$ and $H_{s1}$. Thus, by balancing them, $H_{s0}$ and $H_{s1}$ are selected to be equal to 1.2 and 1.5 mm, respectively.

### C. Slot Opening Width

The influence of slot opening width $B_{s0}$ on the average torque and peak-to-peak torque is analyzed, as shown in Fig. 5.

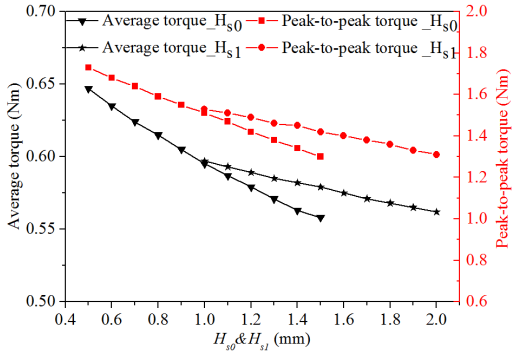


Fig. 4. Average torque and peak-to-peak torque.

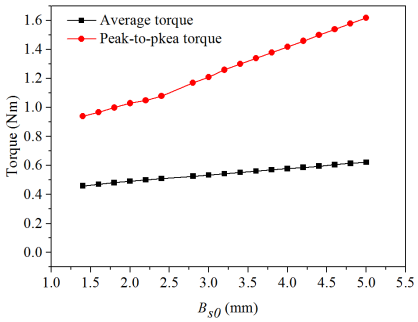


Fig. 5. Torque versus $B_{s0}$.

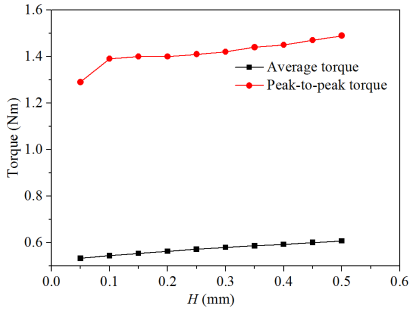


Fig. 6. Torque versus $H$.

It is known that the average torque would increase with the raising of $B_{s0}$, which is caused by the reduction of leakage flux. And the peak-to-peak value of torque is also increasing with $B_{s0}$. The slot opening width is selected to be equal to 3.4 mm.

### *D. Height of Stepped Air Gap*

The curves of average torque and peak-to-peak torque versus height of stepped air gap $H$ are given in Fig. 6. It is known that both the average and peak-to-peak torque would rise with the increasing of $H$. However, the torque ripple, as defined by (4), could reach the minimum when $H$ is equal to 0.4 mm. Thus, $H$ is decided as 0.4 mm in this paper

$$K = \frac{T_{pk2pk}}{T_{\text{avg}}} * 100\% \tag{4}$$

where $K$ is the torque ripple coefficient, $T_{\text{avg}}$ is the average torque, and $T_{pk2pk}$ is the peak-to-peak torque.

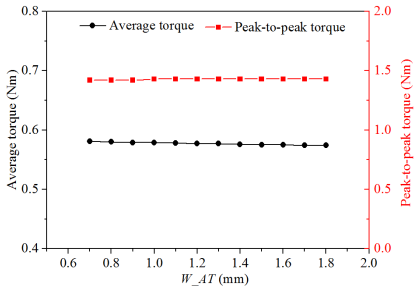


Fig. 7. Torque versus W_AT curves.

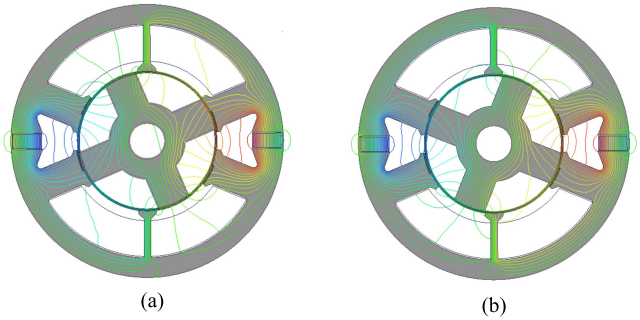


Fig. 8. Rotor position. (a) $\theta = 0°$. (b) $\theta = 45°$.

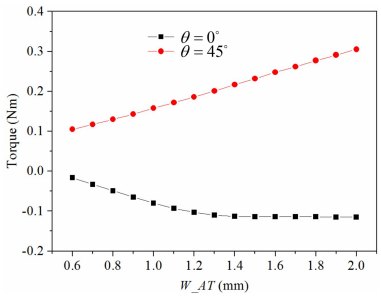


Fig. 9. Starting torque versus W_AT curves.

### *E. Auxiliary Teeth Width*

The influence of auxiliary teeth width, W_AT, on the average and peak-to-peak torque is studied. According to Fig. 7, it is known that the average torque would decrease slightly with the increasing of auxiliary teeth width and W_AT has little influence on the peak-to-peak value.

Defining $\theta = 0°$ and $\theta = 45°$ as the rotor balance positions, as shown in Fig. 8(a) and (b), the torque reaches the minimum value. The corresponding starting torque under rated current versus W_AT curves for both positions is given in Fig. 9. It is known that the starting torque would increase with the rising of W_AT at both $\theta = 0°$ and $\theta = 45°$. The width of auxiliary tooth is selected as 1.2 mm by considering the average and starting torque.

### *F. Optimal Parameters*

The optimal structure parameters for the pole shoe, stepped air gap, and auxiliary tooth are shown in Table II.

TABLE II
OPTIMAL STRUCTURE PARAMETERS

| Symbols | Description | Value | Unit |
|---|---|---|---|
| $H_{s0}$ | Slot opening height | 1.2 | mm |
| $H_{s1}$ | Slot wedge height | 1.5 | mm |
| $B_{s0}$ | Slot opening width | 3.4 | mm |
| $H$ | Height of stepped air gap | 0.4 | mm |
| $W\_AT$ | Width of auxiliary tooth | 1.2 | mm |

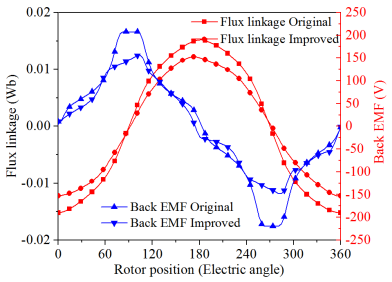


Fig. 10. No-load flux linkage and back EMF.

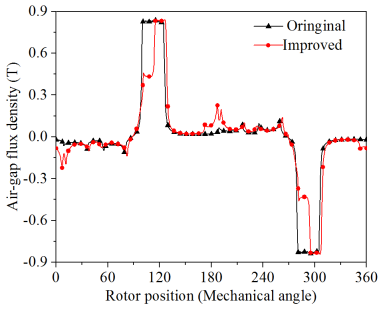


Fig. 11. No-load air-gap flux density.

## IV. PERFORMANCE COMPARISON

### A. No-Load Back EMF and Air-Gap Flux Density

The no-load flux linkage and back EMF (electromotive force) for both machines are given in Fig. 10. It is known that the flux linkage and back EMF of the improved structure are slightly lower than those of the original one. The amplitudes of air-gap flux density of both machines are almost the same, about 0.84 T, as shown in Fig. 11. However, the air-gap flux density curve of the improved structure is different from that of the original one, which is caused by the auxiliary teeth and stepped air gap.

### B. Starting Torque

To compare the starting capability of the original and improved machines, the torque at the starting position under different currents is calculated, as shown in Figs. 12 and 13. It is known that benefiting from the auxiliary teeth and stepped air gap, the starting torque of the improved structure is much higher than that of the original one.

### C. Electromagnetic Torque

It is known that the introduction of pole shoe and auxiliary teeth will lead to the increasing of leakage flux and reduction

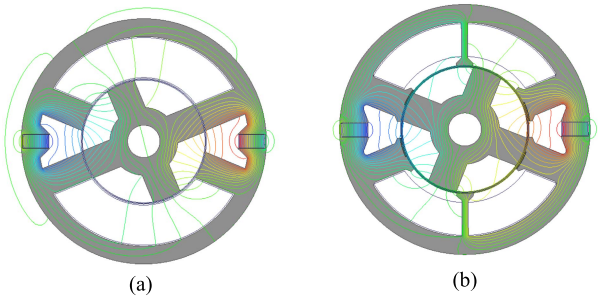


Fig. 12. Flux at the start position for both machines. (a) Original machine. (b) Improved machine.

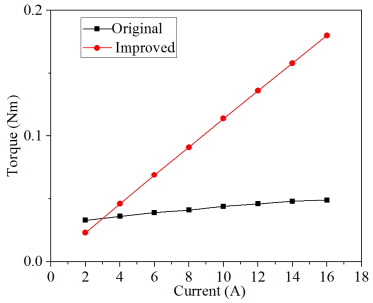


Fig. 13. Starting torque under different currents.

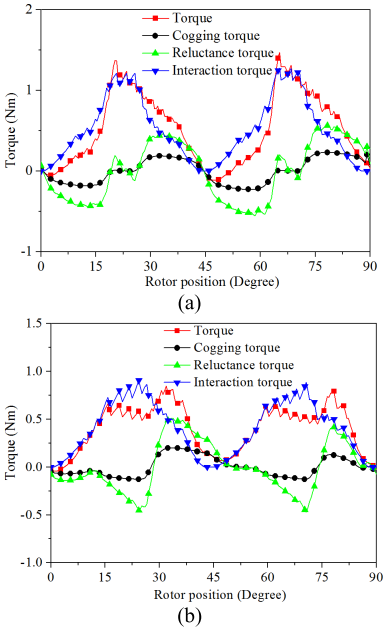


Fig. 14. Torque components. (a) Original. (b) Improved.

of no-load flux linkage inevitably. Besides, the equivalent air-gap length is also increased due to the introduced stepped air gap, which results the further decreasing of no-load flux linkage, as shown in Fig. 10. Thus, the average electromagnetic torque of the improved structures (0.52 Nm) is 21.2% lower than that of the original one (0.41 Nm), as given in Fig. 14. However, the peak-to-peak torque of the original and improved structures are 1.59 and 0.89 Nm, respectively. Thus, the torque ripple for the improved topology is 44% lower

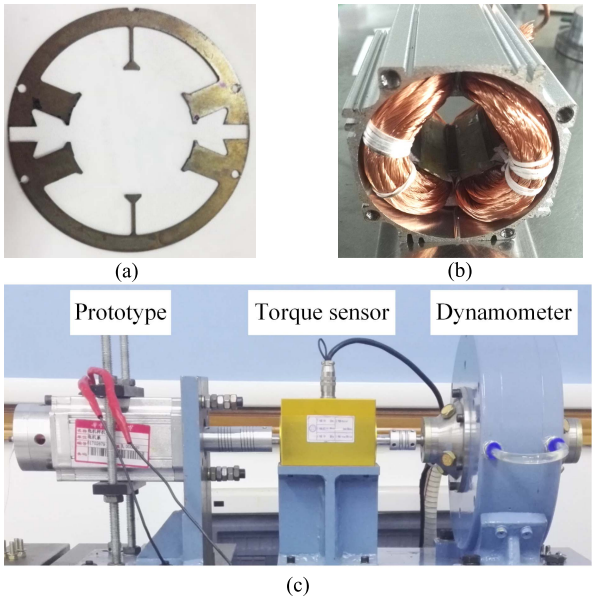


Fig. 15. Prototype and test bed. (a) Stator lamination. (b) Stator and winding. (c) Test bed.

than that of original one though the average torque is 21.1% lower.

To further investigate the influence of the pole shoe, stepped air gap, and auxiliary teeth on the electromagnetic torque, the interaction, reluctance, and cogging torque of the original and improved structures are analyzed based on (3), as shown in Fig. 14. It is known that compared with the original machine, the value of reluctance torque for the improved structure is higher at rotor position 0° and 45°, and reaches the minimum value at 22.5° and 67.5°, where the interaction torque reaches its maximum. Thus, the minimal torque could be increased and the torque ripple could be improved. Besides, the cogging torque of the improved topology is 0.33 Nm, which is 28.3% lower than that of the original one, 0.46 Nm. Thus, the torque ripple of the improved structure can be further reduced.

## V. Experiment

To verify the feasibility of the proposed machine, a prototype is manufactured and the specifications are kept as the same as those in Tables I and II. The stator lamination of the prototype and test bed are shown in Fig. 15.

The starting torque with different currents, no-load back EMF at 1730 rpm, and static torque with 12 A phase current are tested, as shown in Fig. 16. It demonstrates that the measured results are in good agreement with those calculated by 2-D FEA within considerable errors, which is mainly caused by the non-linearity of the magnetic circuit, ignorance of end effect, and machining and measurement errors.

The efficiencies (the operation speed is below 5000 rpm due to the limitation of test bed) of this prototype are measured, and it demonstrates that the highest efficiency (84.2%) could be obtained when the operation speed is 4553 rpm and the given current is 8.1 A, as shown in Table III.

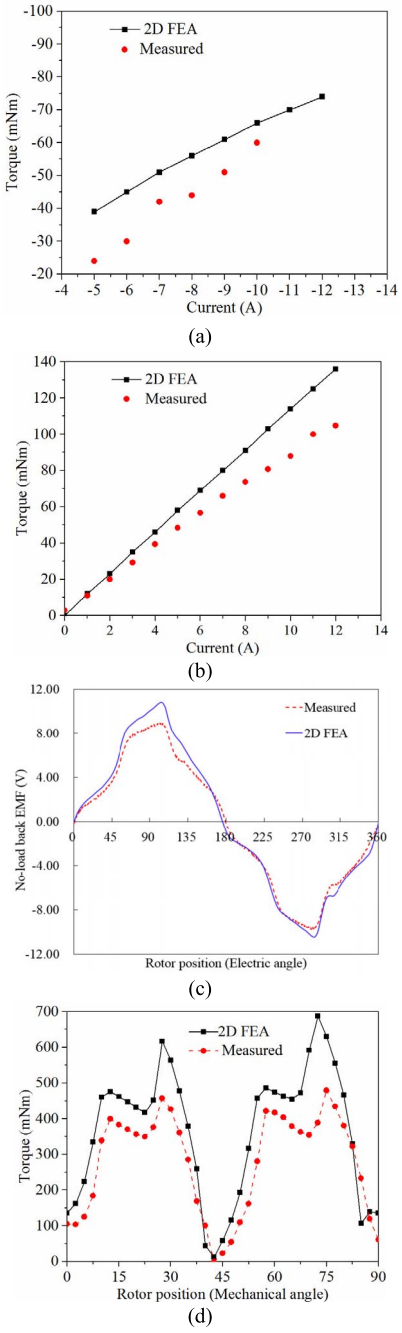


Fig. 16. Starting torque and static torque. (a) Starting torque at $\theta = 0°$. (b) Starting torque at $\theta = 45°$. (c) No-load back EMF. (d) Static torque.

TABLE III
Efficiency and Other Electromagnetic Indexes

| Speed (rpm) | Current (A) | Torque (mNm) | Input power (W) | Output Power (W) | Efficiency (%) |
|---|---|---|---|---|---|
| 4,553 | 8.1 | 168.2 | 95.2 | 80.2 | 84.2 |

## VI. Conclusion

An improved 4/4 stator/rotor SP-ASPDSPMM is proposed in this paper. The special topology and operation principle are investigated. The effect of designed structure parameters on the electromagnetic torque is analyzed based on 2-D FEA. The performance comparison of main electromagnetic performance indexes between the original and improved structures is made.

It indicates that the average torque, cogging torque, and torque ripple of the improved topology are 21.1%, 28.3%, and 44% lower than those of the original one, respectively. Besides, the starting torque of the improved machine is also higher than that of the original one. One prototype for the improved structure is made and the starting torque with different currents, static torque under the given current, and no-load back EMF are measured. It indicates that the experimental results are in good agreement with theoretical analysis based on 2-D FEA with considerable errors.

## ACKNOWLEDGMENT

This work was supported by the National Natural Science Foundation of China under Grant 51577076.

## REFERENCES

[1] M. Cheng, W. Hua, J. Zhang, and W. Zhao, "Overview of stator permanent magnet brushless machines," *IEEE Trans. Ind. Electron.*, vol. 58, no. 11, pp. 5087–5101, Nov. 2011.

[2] K. T. Chau, C. C. Chan, and C. Liu, "Overview of permanent-magnet brushless drives for electric and hybrid electric vehicles," *IEEE Trans. Ind. Electron.*, vol. 55, no. 6, pp. 2246–2257, Jun. 2008.

[3] D. A. Staton, R. P. Deodhar, W. L. Soong, and T. J. E. Miller, "Torque prediction using the flux-MMF diagram in AC, DC, and reluctance motors," *IEEE Trans. Ind. Appl.*, vol. 32, no. 1, pp. 180–188, Jan./Feb. 1996.

[4] A. S. Isfanuti *et al.*, "Small single-phase two pole ferrite-PM-stator double-saliency motor: Optimal design and experimental characterization," in *Proc. 22nd Int. Conf. Electr. Mach. (ICEM)*, Sep. 2016, pp. 2492–2500.

[5] S. Bentouati, Z. Q. Zhu, and D. Howe, "Influence of design parameters on the starting torque of a single-phase PM brushless DC motor," *IEEE Trans. Magn.*, vol. 36, no. 5, pp. 3533–3536, Sep. 2000.

[6] A. S. Icfanuti, L. N. Tutelea, F. J. H. Kalluf, and I. Boldea, "A novel design of stator ferrite PM single phase doubly salient small motor: FEM characterization and controlled dynamics," in *Proc. Int. Conf. Optim. Electr. Electron. Equip. (OPTIM)*, May 2014, pp. 284–290.

[7] Y. Liao, F. Liang, and T. A. Lipo, "A novel permanent magnet motor with doubly salient structure," *IEEE Trans. Ind. Appl.*, vol. 31, no. 5, pp. 1069–1078, Sep. 1995.

[8] B. Dunxin and Z. Qionghua, "A novel single phase doubly salient permanent magnet motor," in *Proc. IEEE Int. Conf. Power Electron. Drive Syst. (PEDS)*, Jul. 1999, pp. 725–729.

[9] J. Z. Zhang, M. Cheng, and Y. Zhang, "Single phase doubly salient permanent magnet generator with full-pitched winding," in *Proc. IEEE Int. Electr. Mach. Drives Conf. (IEMDC)*, May 2009, pp. 311–316.

[10] M. He, W. Xu, and C. Ye, "Novel 4/4 stator/rotor single-phase asymmetric-stator-pole doubly salient permanent magnet machine," in *Proc. Int. Conf. Energy Convers. Congr. Expo. (ECCE)*, Oct. 2017, pp. 5049–5056.